m_J mixing and multipole relaxation in $6\,^2P$ rubidium atoms induced by He, Ne, and Ar collisions

W. Kedzierski, R. B. Middleton, and L. Krause
Department of Physics, University of Windsor, Windsor, Ontario, Canada N9B 3P4
(Received 2 July 1990; revised manuscript received 17 September 1990)

Rubidium vapor, contained together with a buffer gas in a quartz cell located in a 4.75-T magnetic field, was irradiated with light from a pulsed dye laser producing selective excitation of each $6\,^2P$ Zeeman substate in turn. Collisions of the excited and polarized atoms with the ground-state He, Ne, or Ar atoms and the resulting Zeeman mixing produced a population of the whole Zeeman manifold and resulted in the emission of a Zeeman fluorescence spectrum that was resolved with a scanning Fabry-Pérot interferometer and recorded with a photomultiplier and a multichannel scaler. Measurements of the relative intensities of the fluorescence components in relation to the buffer-gas pressures yielded the absolute (thermally averaged) cross sections for Zeeman mixing and cross sections for relaxation of the atomic multipole moments for collisions with He, Ne, and Ar.

We have recently described an experimental study of relaxation of the atomic dipole, quadrupole, and octupole moments in $5\,^2P$ potassium atoms, induced in collisions with ground-state He, Ne, and Ar atoms.[1,2] The experiments were carried out in a high magnetic field and yielded cross sections which agreed well with values predicted by concurrent calculations performed elsewhere.[3,4] We now report the results of experiments in which we excited each sublevel of the Rb $6\,^2P$ Zeeman manifold in turn and investigated the relative intensities of all the Zeeman components of the resulting fluorescence spectrum in relation to the densities of the buffer gases, obtaining cross sections for all the possible collision-induced transitions between the Zeeman sublevels and for the relaxation of the atomic multipole moments.

When a rubidium atom, excited to a $6\,^2P_{J,m}$ Zeeman substate, collides with a noble-gas atom, it may be transferred to another m_J substate. Because of the moderate $6\,^2P$ fs splitting, the collisional transfer will span all six Zeeman substates of the $6\,^2P$ manifold. Since the initial excitation of a single m_J substate produces a bulk multipole moment in the vapor-gas mixture, the collisional m_J mixing is equivalent to the collisional relaxation of the various multipole moments: the dipole (orientation), quadrupole (alignment), and octupole.[5,6] The multipole relaxation cross sections $\Lambda^{(1)}_{1/2}$ and $\Lambda^{(L)}_{3/2}$ $(L=1,2,3)$ may be expressed in terms of the Zeeman mixing cross sections $Q(J,m\rightarrow J',m')$ by Eqs. (4)–(7) in Ref. 2 or by the following equivalent transformation equations which take advantage of additional Zeeman mixing cross sections,[7,8] and are based on the assumption that $Q(J,m\rightarrow J',m)=Q(J,-m\rightarrow J',-m)$:

$$\Lambda^{(1)}_{1/2}=2Q(\tfrac{1}{2},\tfrac{1}{2}\rightarrow\tfrac{1}{2},-\tfrac{1}{2})\ , \tag{1}$$

$$\Lambda^{(1)}_{3/2}=\tfrac{1}{5}Q(\tfrac{3}{2},-\tfrac{1}{2}\rightarrow\tfrac{3}{2},\tfrac{1}{2})+\tfrac{8}{5}Q(\tfrac{3}{2},-\tfrac{3}{2}\rightarrow\tfrac{3}{2},\tfrac{1}{2}) +\tfrac{9}{5}Q(\tfrac{3}{2},-\tfrac{3}{2}\rightarrow\tfrac{3}{2},\tfrac{3}{2})+\tfrac{2}{5}Q(\tfrac{3}{2},\tfrac{3}{2}\rightarrow\tfrac{3}{2},\tfrac{1}{2})\ , \tag{2}$$

$$\Lambda^{(2)}_{3/2}=2Q(\tfrac{3}{2},-\tfrac{3}{2}\rightarrow\tfrac{3}{2},\tfrac{1}{2})+2Q(\tfrac{3}{2},\tfrac{3}{2}\rightarrow\tfrac{3}{2},\tfrac{1}{2})\ , \tag{3}$$

$$\Lambda^{(3)}_{3/2}=\tfrac{9}{5}Q(\tfrac{3}{2},-\tfrac{1}{2}\rightarrow\tfrac{3}{2},\tfrac{1}{2})+\tfrac{2}{5}Q(\tfrac{3}{2},-\tfrac{3}{2}\rightarrow\tfrac{3}{2},\tfrac{1}{2}) +\tfrac{1}{5}Q(\tfrac{3}{2},-\tfrac{3}{2}\rightarrow\tfrac{3}{2},\tfrac{3}{2})+\tfrac{8}{5}Q(\tfrac{3}{2},\tfrac{3}{2}\rightarrow\tfrac{3}{2},\tfrac{1}{2})\ . \tag{4}$$

The Zeeman mixing cross sections are defined analogously with the gas-kinetic cross section

$$\gamma(J,m\rightarrow J',m')=NvQ(J,m\rightarrow J',m')\ , \tag{5}$$

where $\gamma(J,m\rightarrow J',m')$ represents the rate of transfer between the Zeeman substates within the $6\,^2P$ manifold. N is the density of the buffer-gas atoms and v is the average relative speed of the colliding atoms. Under single-collision conditions, when an excited Rb atom undergoes at most one inelastic collision during its lifetime,[9]

$$Q(J,m\rightarrow J',m')=(1/Nv\tau)(N_{J',m'}/N_{J,m})\ , \tag{6}$$

where $N_{J,m}$ represents the population of a Zeeman substate and $\tau=11.5\times10^{-8}$ s is the mean radiative lifetime of the $6\,^2P$ state [this is an average of $\tau_{1/2}=11.68\times10^{-8}$ s (Ref. 10) and $\tau_{3/2}=11.4\times10^{-8}$ s (Ref. 11)]. Since in this experiment only circularly polarized fluorescence was detected, the population ratios are proportional to the ratios of the measured integrated intensities of the fluorescence components:

$$\frac{N_{J,m}}{N_{J',m'}}=\frac{I_{J,m}}{I_{J',m'}}\frac{A^{\sigma}_{J',m'}}{A^{\sigma}_{J,m}}\ , \tag{7}$$

where $A^{\sigma}_{J,m}$ are the appropriate Einstein A coefficients for decay of the excited states by emission of circularly polarized light,[12] which are magnetic-field dependent. In a field of 4.75 T they are in the ratio[8]

$$A^{\sigma}_{3/2\pm3/2}:A^{\sigma}_{3/2\pm1/2}:A^{\sigma}_{1/2\pm1/2}=3.00:0.97:2.01\ . \tag{8}$$

Equations (1)–(7) are used to derive the multipole relaxation cross sections from the integrated intensities of the Zeeman fluorescence components, measured in relation to the buffer-gas densities.

The apparatus and experimental procedure have been described previously[1] and were used in this investigation

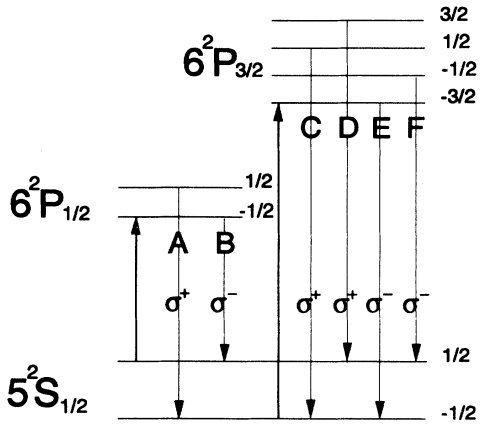

FIG. 1. Schematic diagram of the σ transitions between the $5\,^2S$ and $6\,^2P$ Zeeman substates in rubidium. Only the B and E excitations are indicated; the π transitions are not shown.

with minor changes. Rubidium vapor together with a noble gas was contained in a quartz fluorescence cell placed in a 4.75-T magnetic field and was irradiated with dye-laser pulses tuned to selectively excite each Zeeman substate of the $6\,^2P$ manifold in turn. The resulting circularly polarized fluorescence, which was observed along the direction perpendicular to the direction of excitation and parallel to the magnetic field, consisted of a direct fluorescence component emitted from the optically excited Zeeman substate and sensitized components emitted from the substates populated by collisions. The fluorescence spectrum, which consisted of σ^+ and σ^- components identified in Fig. 1, was resolved with a piezoelectrically scanned Fabry-Pérot interferometer whose output was detected with a photomultiplier and accumulated in a multichannel scaler.

Figure 2 shows a representative trace of the fluorescence spectrum obtained with $6\,^2P_{3/2,-3/2}$ excitation in the presence of 120 mTorr Ar. The fluorescence peaks are identified as arising from the transitions labeled $A-F$ in Fig. 1. The intensity pattern in the spectrum suggests that Zeeman mixing within the $^2P_{3/2}\,fs$ state is considerably more efficient than mixing between the fs states.

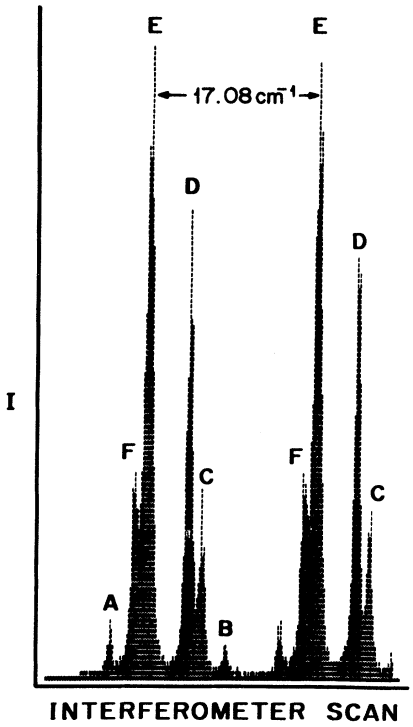

FIG. 2. A trace of the Zeeman fluorescence spectrum emitted from rubidium vapor mixed with 120 mTorr Ar. The $6\,^2P_{3/2,-3/2}$ state was optically excited and the peaks are labeled to correspond to the transitions indicated in Fig. 1. The free spectral range of the interferometer was 17.08 cm^{-1}.

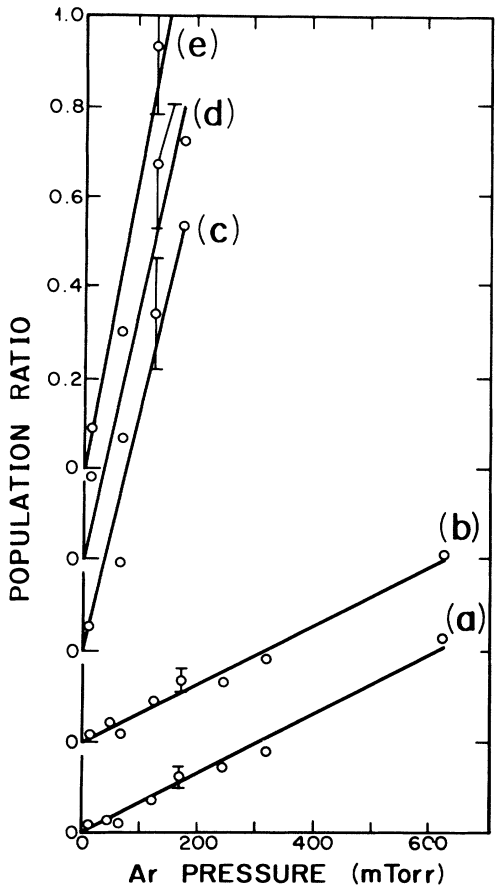

FIG. 3. Plots of Zeeman fluorescence intensity (and population) ratios, arising from $6\,^2P_{3/2,3/2}$ excitation, showing effects of Zeeman mixing by Rb-Ar collisions. The separate origin for each plot is indicated on the vertical axis. The error bars represent statistical scatter of the measurements. Each point represents the intensity ratio of the specified components, multiplied by the ratio of the appropriate $A^{\sigma}_{J,m}$ coefficients. (a) $I(A)/I(D)$, (b) $I(B)/I(D)$, (c) $I(E)/I(D)$, (d) $I(C)/I(D)$, (e) $I(F)/I(D)$.

TABLE I. $6\,^2P$ Zeeman mixing cross sections (10^{-16} cm^2). Dashes indicate that the relevant fluorescence component was not adequately resolved.

Designation $Q(J,m\rightarrow J',m')$	Collision partner He	Ne	Ar
$Q(\frac{3}{2},+\frac{1}{2}\rightarrow\frac{1}{2},+\frac{1}{2})$	50±13	9±2.5	16±5
$Q(\frac{3}{2},+\frac{1}{2}\rightarrow\frac{1}{2},-\frac{1}{2})$	45±13	9±3	16±5
$Q(\frac{3}{2},+\frac{1}{2}\rightarrow\frac{3}{2},+\frac{3}{2})$	438±85	140±30	218±45
$Q(\frac{3}{2},+\frac{1}{2}\rightarrow\frac{3}{2},-\frac{3}{2})$	521±100	163±30	155±30
$Q(\frac{3}{2},+\frac{1}{2}\rightarrow\frac{3}{2},-\frac{1}{2})$	334±65	136±30	140±30
$Q(\frac{3}{2},+\frac{3}{2}\rightarrow\frac{1}{2},+\frac{1}{2})$	76±24	16±5	32±9
$Q(\frac{3}{2},+\frac{3}{2}\rightarrow\frac{1}{2},-\frac{1}{2})$	–	17±5	32±9
$Q(\frac{3}{2},+\frac{3}{2}\rightarrow\frac{3}{2},+\frac{1}{2})$	–	–	292±115
$Q(\frac{3}{2},+\frac{3}{2}\rightarrow\frac{3}{2},-\frac{3}{2})$	–	244±50	272±100
$Q(\frac{3}{2},+\frac{3}{2}\rightarrow\frac{3}{2},-\frac{1}{2})$	–	296±60	343±120
$Q(\frac{3}{2},-\frac{3}{2}\rightarrow\frac{1}{2},+\frac{1}{2})$	42.0±20; 10.4[a]	–	34±15
$Q(\frac{3}{2},-\frac{3}{2}\rightarrow\frac{1}{2},-\frac{1}{2})$	31±9; 6.2[a]	–	22±7
$Q(\frac{3}{2},-\frac{3}{2}\rightarrow\frac{3}{2},+\frac{1}{2})$	378±75; 147.1[a]	187±35	285±50
$Q(\frac{3}{2},-\frac{3}{2}\rightarrow\frac{3}{2},+\frac{3}{2})$	283±55; 71.5[a]	185±35	212±105
$Q(\frac{3}{2},-\frac{3}{2}\rightarrow\frac{3}{2},-\frac{1}{2})$	425±210; 165[a]	311±90	374±180
$Q(\frac{3}{2},-\frac{1}{2}\rightarrow\frac{1}{2},+\frac{1}{2})$	49±10; 9.1[a]	9±2.5	12±3.5
$Q(\frac{3}{2},-\frac{1}{2}\rightarrow\frac{1}{2},-\frac{1}{2})$	39±10; 7.6[a]	8±2.5	11±3
$Q(\frac{3}{2},-\frac{1}{2}\rightarrow\frac{3}{2},+\frac{1}{2})$	287±80; 94.9[a]	129±25	115±30
$Q(\frac{3}{2},-\frac{1}{2}\rightarrow\frac{3}{2},+\frac{3}{2})$	341±100; 147.1[a]	159±30	–
$Q(\frac{3}{2},-\frac{1}{2}\rightarrow\frac{3}{2},-\frac{3}{2})$	492±50; 165[a]	174±35	–
$Q(\frac{1}{2},+\frac{1}{2}\rightarrow\frac{1}{2},-\frac{1}{2})$	129±40	27±8	34±10
$Q(\frac{1}{2},+\frac{1}{2}\rightarrow\frac{3}{2},+\frac{1}{2})$	46±15	7±2	14±4
$Q(\frac{1}{2},+\frac{1}{2}\rightarrow\frac{3}{2},+\frac{3}{2})$	51±20	6±1	14±3
$Q(\frac{1}{2},+\frac{1}{2}\rightarrow\frac{3}{2},-\frac{3}{2})$	58±20	8±1.5	22±6
$Q(\frac{1}{2},+\frac{1}{2}\rightarrow\frac{3}{2},-\frac{1}{2})$	51±10	–	21±5
$Q(\frac{1}{2},-\frac{1}{2}\rightarrow\frac{1}{2},+\frac{1}{2})$	83±40; 49.4[a]	28±8	35±10
$Q(\frac{1}{2},-\frac{1}{2}\rightarrow\frac{3}{2},+\frac{1}{2})$	20±6; 6.8[a]	9±2.5	20±5
$Q(\frac{1}{2},-\frac{1}{2}\rightarrow\frac{3}{2},+\frac{3}{2})$	23±5; 7.9[a]	7±1.5	16±3
$Q(\frac{1}{2},-\frac{1}{2}\rightarrow\frac{3}{2},-\frac{3}{2})$	25±5; 4.7[a]	7±2	17±3
$Q(\frac{1}{2},-\frac{1}{2}\rightarrow\frac{3}{2},-\frac{1}{2})$	25±5; 5.8[a]	7±1.5	17±5

[a]Reference 3.

The ratios of the sensitized-to-direct integrated intensities in the many fluorescence spectra were multiplied by the appropriate ratios of the $A^{\sigma}_{J,m}$ coefficients and are plotted against buffer-gas pressures in Fig. 3, which represents a typical plot of population ratios of collisionally-to-directly (optically) populated Zeeman sublevels in the $6\,^2P$ Zeeman manifold. The linearity of the plots suggests the absence of multiple collisional transfers including back transfer, and was also noted in all the additional data that are not shown here. The Zeeman mixing cross sections were calculated by substituting the data in Eq. (7) and subjecting them to a weighted linear regression fit

TABLE II. $6\,^2P$ multipole relaxation cross sections (10^{-16} cm^2).

Designation	Collision partner He	Ne	Ar
$\Lambda^{(1)}_{1/2}$	212±100	55±15	69±19
$\Lambda^{(1)}_{3/2}$	1348±345	805±170	1015±380
$\Lambda^{(2)}_{3/2}$	1606±570	996±250	1236±430
$\Lambda^{(3)}_{3/2}$	1457±1050	1041±410	1091±830

over the range of buffer-gas pressures where the population ratios remained linear with $Nv\tau$. The cross sections are listed in Table I and it may be seen that, in all cases, the cross sections are largest for He and smallest for Ne, a trend which has also been observed in other experiments.[1,2,9] The cross sections for m_J mixing between the $^2P_{1/2}$ and $^2P_{3/2}$ fs states are smaller than the mixing cross sections within the $^2P_{1/2}$ state, which are again smaller than the cross sections for mixing within the $^2P_{3/2}$ state. This was to be expected since the $6\,^2P$ fs splitting (77 cm^{-1}) is relatively large and, while it is smaller than kT at the temperature of the fluorescing vapor-gas mixture (269 cm^{-1}), it is non-negligible compared to the inverse collision time. That the cross sections for m_J mixing within the $^2P_{1/2}$ state are significantly smaller than within the $^2P_{3/2}$ state may be due to the $m_J \leftrightarrow -m_J$ transitions being forbidden, as has been indicated in some earlier theoretical studies.[13–15] On the other hand, it has been suggested that these transitions are made possible by magnetic-field-induced $^2P_{1/2}$-$^2P_{3/2}$ mixing, a process which has been found to be magnetic-field dependent.[16] Table I also includes some theoretical cross sections[3] which are clearly smaller than the experimental values, though the trends are in agreement. These various properties of the Zeeman mixing cross sections are reflected in the cross sections for relaxation of the multipole moments that were derived from the m_J mixing cross sections and are listed in Table II.

This research was supported by a grant from the Natural Sciences and Engineering Research Council of Canada.

[1]R. W. Berends, W. Kedzierski, and L. Krause, Phys. Rev. A **37**, 68 (1988).

[2]R. W. Berends, W. Kedzierski, W. E. Baylis, and L. Krause, Phys. Rev. A **39**, 1526 (1989).

[3]J. Pascale (private communication); see also *Abstracts of Contributed Papers, Thirteenth International Conference on the Physics of Electronic and Atomic Collisions, Berlin, 1983, edited by* J. Eichler, W. Fritsch, I. V. Hertel, N. Stolterfoht, and U. Wille (ICPEAC, Berlin, 1984).

[4]A. Spielfiedel and N. Feautrier (private communication).

[5]R. B. Bulos and W. Happer, Phys. Rev. A **4**, 849 (1971).

[6]W. E. Baylis, in *Progress in Atomic Spectroscopy, Part B,* edited by W. Hanle and H. Kleinpoppen (Plenum, New York, 1979).

[7]W. Berdowski, T. Shiner, and L. Krause, Phys. Rev. A **4**, 984 (1971).

[8]R. Boggy and F. A. Franz, Phys. Rev. A **25**, 1887 (1982).

[9]P. Skalinski and L. Krause, Phys. Rev. A **26**, 3338 (1982).

[10]J. H. Gallagher, Ph.D. thesis, University of Colorado, Boulder, Colorado, 1969.

[11]H. Bucka, B. Grossivendt, and H. A. Schuessler, Z. Phys. **194**, 193 (1966).

[12]A. C. G. Mitchell and M. W. Zemansky, *Resonance Radiation and Excited Atoms* (Cambridge University Press, Cambridge, England, 1934).

[13]F. A. Franz and J. R. Franz, Phys. Rev. **148**, 82 (1966).

[14]F. A. Franz, G. Leutert, and R. Shuey, Helv. Phys. Acta **40**, 779 (1967).

[15]M. Elbel and F. Naumann, Z. Phys. **204**, 501 (1967).

[16]J. Guiry and L. Krause, Phys. Rev. A **12**, 2407 (1975).